All-loop Mondrian reduction of 4-particle amplituhedron at positive infinity

Junjie Rao

Max Planck Institute for Gravitational Physics (Albert Einstein Institute), 14476 Potsdam, Germany

Abstract

This article introduces a systematic framework to understand (not to derive yet) the all-loop 4-particle amplituhedron in planar $\mathcal{N}=4$ SYM, utilizing both positivity and the Mondrian diagrammatics. Its key idea is the simplest one so far: we can decouple one or more sets of loop variables (x, y, z, w) from the rest by just setting these variables to either zero or infinity so that their relevant positivity conditions are trivialized, then the all-loop consistency requires that we get lower loop amplituhedra as "residues". These decoupling relations connect higher loop DCI integrals with the lower ones, enabling us to identify their coefficients starting from the 3-loop case. And surprisingly, the delicate mechanism of this process is the simple Mondrian rule $D = X + Y$, which forces those visually non-Mondrian DCI integrals to have the correct coefficients such that the amplituhedron can exactly reduce to the lower loop one. Examples cover all DCI integrals at $L=3, 4, 5, 6$, especially, the subtle 6-loop coefficients $+2$ and 0 are neatly explained in this way.

Contents

E-mail address: jrao@aei.mpg.de.

1. Introduction

The amplituhedron proposal of planar $\mathcal{N}=4$ SYM [1,2] is a novel reformulation which only uses positivity conditions for all physical poles to construct the amplitude or integrand. For given (n, k, L) where n is the number of external particles, $(k+2)$ is the number of negative helicities and L is the loop order, the most generic loop amplituhedron is defined via

$$Y_\alpha^I = C_{\alpha a} Z_a^I, \quad \mathcal{L}_{(i)\alpha}^I = D_{(i)\alpha a} Z_a^I, \tag{1.1}$$

here $C_{\alpha a}$ is the $(k \times n)$ positive Grassmannian encoding the tree-level information and $D_{(i)\alpha a}$ is the $(2 \times n)$ positive Grassmannian with respect to the i-th loop, and Z_a^I is the kinematical data made of n generalized $(k+4)$-dimensional momentum twistors, which also obeys positivity as

$$\langle Z_{a_1} \ldots Z_{a_{k+4}} \rangle > 0 \ \text{ for } \ a_1 < \ldots < a_{k+4}, \tag{1.2}$$

then the overall constraint is, all ordered minors of the matrix

$$\begin{pmatrix} D_{(i_1)} \\ \vdots \\ D_{(i_l)} \\ C \end{pmatrix} \tag{1.3}$$

are positive for any collection of D's with $0 \leq l \leq L$. Through this positive constraint we can construct the $d\log$ form encoding logarithmic singularities of the loop amplituhedron. In practice, we also need to know how to explicitly triangulate this geometric object, and the most recent sign-flip picture introduced in [3] gives a detailed prescription. However, in this work we will focus on the simplest all-loop case of only four particles, and hence we don't need to use the sign flips.

In general, based on the definitions above, we require all physical poles to be positive:

$$\langle YZ_i Z_{i+1} Z_j Z_{j+1} \rangle > 0, \quad \langle Y\mathcal{L}_{(i)} Z_j Z_{j+1} \rangle > 0, \quad \langle Y\mathcal{L}_{(i)}\mathcal{L}_{(j)} \rangle > 0, \tag{1.4}$$

but for the special 4-particle loop amplituhedron, there is only one sector: the MHV sector (or anti-MHV equivalently) of $k=0$, and these constraints simplify to

$$\langle 1234 \rangle > 0, \quad \langle \mathcal{L}_{(i)} Z_j Z_{j+1} \rangle > 0, \quad \langle \mathcal{L}_{(i)}\mathcal{L}_{(j)} \rangle > 0, \tag{1.5}$$

as there is no Y component. We can further choose the simple positive data, and parameterize D's with positive variables (x_i, y_i, z_i, w_i) as

$$(Z_1, Z_2, Z_3, Z_4) = \begin{pmatrix} 1 & 0 & 0 & 0 \\ 0 & 1 & 0 & 0 \\ 0 & 0 & 1 & 0 \\ 0 & 0 & 0 & 1 \end{pmatrix}, \quad D_{(i)} = \begin{pmatrix} 1 & x_i & 0 & -w_i \\ 0 & y_i & 1 & z_i \end{pmatrix}, \tag{1.6}$$

such that $\langle \mathcal{L}_{(i)} Z_j Z_{j+1} \rangle > 0$ can be trivialized as (note the twisted cyclicity $Z_{4+1} = -Z_1$)

$$\langle \mathcal{L}_{(i)} 12 \rangle = w_i, \ \ \langle \mathcal{L}_{(i)} 23 \rangle = z_i, \ \ \langle \mathcal{L}_{(i)} 34 \rangle = y_i, \ \ \langle \mathcal{L}_{(i)} 14 \rangle = x_i, \tag{1.7}$$

and the only nontrivial constraint is

$$\langle \mathcal{L}_{(i)} \mathcal{L}_{(j)} \rangle = \det \begin{pmatrix} 1 & x_i & 0 & -w_i \\ 0 & y_i & 1 & z_i \\ 1 & x_j & 0 & -w_j \\ 0 & y_j & 1 & z_j \end{pmatrix} > 0. \tag{1.8}$$

In summary, for the 4-particle amplituhedron or integrand at L-loop order, we have the mutual positivity condition for any two sets of loop variables labeled by $i, j = 1, \ldots, L$ as

$$\langle \mathcal{L}_{(i)} \mathcal{L}_{(j)} \rangle \equiv D_{ij} = (x_j - x_i)(z_i - z_j) + (y_j - y_i)(w_i - w_j) > 0, \tag{1.9}$$

where positive variables x_i, y_i, z_i, w_i and D_{ij} are all possible physical poles. Though the dominating principle is simple and symmetric up to all loops, as the loop order increases, its calculational complexity grows explosively due to the highly nontrivial intertwining of all $L(L-1)/2$ positivity conditions. Therefore it is more practical to seek new perspectives or techniques other than confronting the direct calculation. This, however, does not imply the direct calculation is impossible, as a better interpretation might redefine the problem so that the meaning of "direct" is more trivialized. This work shows how a simpler problem got complicated, then returns to its plain form after we switch to the correct perspective extracted from all the previous clues. So it is natural to expect the ultimate solution of 4-particle amplituhedron turns out to be even simpler, and hidden elegant patterns like the Mondrian story await to be discovered.

The most recent progress includes the direct calculation of the 3-loop case [4], the all-loop Mondrian diagrammatics [5] for a subset of dual conformally invariant (DCI) loop integrals of which pole structures can be Mondrianized, and the positive cuts [6] as a simplified approach to identify coefficients of a given basis of DCI integrals. This work continues to explore the 4-particle amplituhedron at higher loop orders, as we will introduce a new systematic framework to more clearly integrate positivity with the Mondrian diagrammatics. Note that, though we will use some terminologies already involved in the previous works, such as "Mondrian diagrammatics", in this new setting their meanings are slightly different. To make the current work as self-contained as possible, we will redefine the frequently used terms so it is not necessary to recall them back in [4–6].

The key idea here is straightforward: we can decouple one or more sets of loop variables (x_i, y_i, z_i, w_i) from the rest by setting them to either zero or infinity to trivialize the relevant positivity conditions, then the all-loop consistency requires that we get lower loop amplituhedra as residues. Using these decoupling relations to connect DCI integrals of different loop orders, we can identify coefficients of DCI integrals at $L \geq 4$ starting from the 3-loop case. And it is the simple Mondrian rule $D = X + Y$ that accounts for this delicate mechanism and forces those visually non-Mondrian DCI integrals to have the correct coefficients.

To begin to rebuild everything, forgetting all later advances, we can return to the original definition of this problem [1,2]. First let's introduce a convenient convention for the following derivations: we will use the *dimensionless ratio* as the integrand, for example, in the 2-loop integral [2]
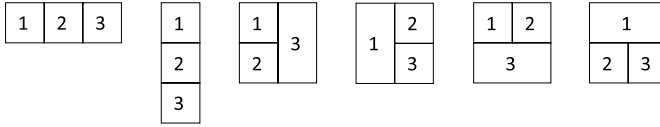
Fig. 1. Diagrams of DCI integrals corresponding to the first six terms in R_3. In our convention, faces x, z, y, w locate at the left, right, top and bottom of the diagram respectively.

$$\int \frac{dx_1}{x_1} \frac{dy_1}{y_1} \frac{dz_1}{z_1} \frac{dw_1}{w_1} \frac{dx_2}{x_2} \frac{dy_2}{y_2} \frac{dz_2}{z_2} \frac{dw_2}{w_2} R \quad \text{where} \quad R = \frac{x_2 z_1 + x_1 z_2 + y_2 w_1 + y_1 w_2}{D_{12}},$$

$$(1.10)$$

R is the integrand we will extensively manipulate. In other words, the full integral is made up of the $d \log$ measure of all positive variables and this ratio R. In particular, the 1-loop integrand is trivially 1 as there is no mutual positivity to be imposed. With this convention, when the integral is evaluated at either zero or infinity with respect to some variables, there is no extra factor to be added to the residual integrand, and the $d \log$ measure of those unfixed variables can be dropped for convenience.

Then what use does this residue evaluation at zero or infinity have, which seems trivial compared to the positive cuts [6]? If we simply set $x_j \to \infty$ and $z_j = 0$ in

$$D_{ij} = (x_j - x_i)(z_i - z_j) + (y_j - y_i)(w_i - w_j) \to \infty z_i + (y_j - y_i)(w_i - w_j), \quad (1.11)$$

D_{ij} becomes trivially positive, since the positivity of z_i is magnified by a positive infinity factor.

Let's be more concrete and immediately look at the 3-loop case: $x_3 \to \infty$ and $z_3 = 0$ lead to

$$D_{i3} \to \infty z_i + (y_3 - y_i)(w_i - w_3), \quad (1.12)$$

so D_{13}, D_{23} are positive, and we may claim that the third loop "decouples" from the rest two loops while positivity of D_{12} remains to be imposed. Now according to the integrands defined above (in terms of the 3-loop result R_3 given in [4], see Fig. 1), namely

$$R_2 = \frac{x_2 z_1 + x_1 z_2 + y_2 w_1 + y_1 w_2}{D_{12}}, \quad (1.13)$$

$$R_3 = \frac{x_2 x_3 z_1 z_2 + y_2 y_3 w_1 w_2}{D_{12} D_{23}}$$

$$+ \frac{x_3^2 z_1 z_2 \, y_2 w_1 + x_2 x_3 z_1^2 \, y_3 w_2 + x_2 z_1 \, y_3^2 w_1 w_2 + x_3 z_2 \, y_2 y_3 w_1^2}{D_{12} D_{13} D_{23}} \quad (1.14)$$

$$+ \text{(5 permutations of 1,2,3)}$$

for $L = 2, 3$, the residue of R_3 at $x_3 = \infty, z_3 = 0$ is exactly R_2! This simple relation reflects the consistency of 4-particle amplituhedron as expected. We can further make it a bit more nontrivial by similarly setting $y_3 = \infty, w_3 = 0$, then

$$D_{i3} = \frac{1}{\varepsilon}(z_i + w_i), \quad (1.15)$$

where the infinitesimal ε is used to characterize the divergence of both x_3 and y_3. Now the same relation $R_3 \to R_2$ also holds but in a more interesting way as we will explain. Both situations above in fact encode the *new* Mondrian diagrammatics: in the first case a rectangle-like loop is removed, while in the second a corner-like loop is removed, as visualized in Fig. 2. For the
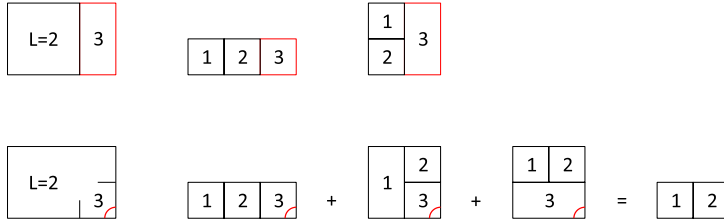
Fig. 2. Rectangle removal $x_3 = \infty$, $z_3 = 0$ and corner removal $x_3 = y_3 = \infty$, $z_3 = w_3 = 0$. Note the rectangle removal is a special (and simplified) inverse operation of the rung rule [7].

rectangle removal, as shown in the 1st line of Fig. 2, two examples of non-vanishing contributions are given, from which the reduction from R_3 to R_2 can be transparently seen. The non-vanishing criterion of a diagram is, its third loop must have contacts with the external faces y, z, w (here we keep using the convention in [4–6], namely faces x, z, y, w locate at the left, right, top and bottom of the diagram respectively). Similarly for the *corner removal*, a diagram must let its third loop have contacts with the external faces z, w in order to be non-vanishing. Of course, the rectangle or corner removal can have different choices of orientation by dihedral symmetry but without loss of generality, we stick to y, z, w and z, w for consistency as above.

However, unlike the rectangle removal for which each 3-loop diagram simply reduces to a 2-loop one, the corner removal leads to more interesting relations among different 3-loop diagrams, as they together reduce to a 2-loop counterpart. As shown in the 2nd line of Fig. 2, after removing the third loop, these three diagrams reduce to the same 2-loop diagram but with various prefactors, of which the sum is unity:

$$\frac{z_2}{z_2 + w_2} + \frac{z_1}{z_1 + w_1} \frac{w_2}{z_2 + w_2} + \frac{w_1}{z_1 + w_1} \frac{w_2}{z_2 + w_2} = 1, \tag{1.16}$$

if we define

$$X_i = \frac{z_i}{z_i + w_i}, \quad Y_i = \frac{w_i}{z_i + w_i}, \quad D_i = X_i + Y_i = 1, \tag{1.17}$$

this is exactly the *Mondrian completeness relation* [5], which is trivial to prove:

$$D_1 X_2 + X_1 Y_2 + Y_1 Y_2 = D_1 D_2. \tag{1.18}$$

Diagrammatically Mondrian factors X_i, Y_i, D_i mean loop 3 has a horizontal contact, vertical contact or no contact with loop $i = 1, 2$ respectively. From these easy examples of two types of loop removal, we see how the Mondrian diagrammatics helps understand the interconnections among different diagrams of various DCI topologies (including their coefficients) in an extremely neat way.

2. Nontrivialities at 4-loop

Next, we are curious to see how this wishfully simple mechanism deals with the more sophisticated 4-loop case, since it involves DCI topologies with coefficient -1 and non-Mondrian pole structure (recall that for a *Mondrian diagram*, all internal lines can be oriented either horizontally or vertically), both of which are absent at lower loop orders. First of all, let's recall the 4-loop DCI topologies as given in Fig. 3.

Here topologies $T_1, \ldots, T_7$ are Mondrian while T_8 is not. As we have known, T_7 and T_8 are associated with coefficient -1, and $T_1, \ldots, T_6$ are associated with $+1$, moreover, T_4 has a D_{ij}
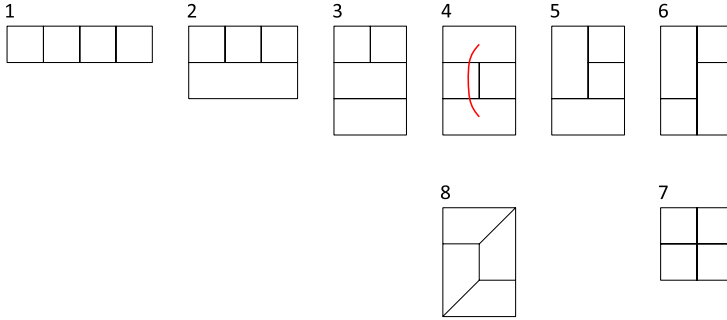
Fig. 3. 4-loop DCI topologies (see [7]). The red curve denotes a rung rule factor D_{ij}, while rung rule factors x, y, z, w are diagrammatically suppressed for convenience. (For interpretation of the colors in the figure(s), the reader is referred to the web version of this article.)
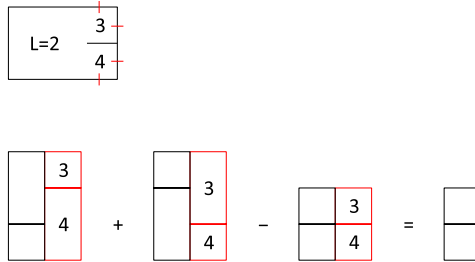

Fig. 4. Block removal and the cancelation between T_6 and T_7 in $R_4 \to R_2$.

factor in the numerator of its integrand. To see why these coefficients are so, we can pretend that they are still unknown yet and denote them by $s_1, \ldots, s_8$. Immediately, we can perform the rectangle removal of loop 4. More rigorously speaking, we impose the limit

$$x_4 = \frac{1}{\varepsilon}, \quad z_4 = 0 \quad \text{where} \quad \varepsilon \to 0 \tag{2.1}$$

in the 4-loop integrand R_4, which takes into account DCI loop integrals of all possible orientations given by dihedral symmetry (the number of which can be 8, 4, 2, or 1 for each topology) and all 4! permutations of loop numbers [7]. Then in the expansion

$$R_4(\varepsilon) = R_4(0) + O(\varepsilon), \tag{2.2}$$

the leading term $R_4(0)$ depends on s_1, s_2, s_3, s_4, s_5 only, and $R_4(0) = R_3$ when $s_1 = s_2 = s_3 = s_4 = s_5 = 1$ as expected. From the Mondrian diagrammatic perspective, this is trivial to understand as a 4-loop example of the rectangle removal. In fact we can further generalize the rectangle to remove more loops at a time, which will justify the existence of T_6, T_7. As visualized in Fig. 4, we now remove a *block* containing loop 3, 4 by imposing

$$x_3 = x_4 = \frac{1}{\varepsilon}, \quad z_3 = z_4 = y_3 = w_4 = 0, \tag{2.3}$$

so that for $i = 1, 2$

$$D_{i3} = D_{i4} = \frac{1}{\varepsilon} z_i, \quad D_{34} = y_4 w_3, \tag{2.4}$$
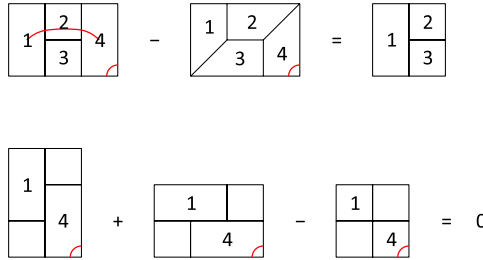
Fig. 5. New features of the 4-loop corner removal.

note that ε helps regularize the expression $(\infty - \infty)$ in D_{34} and renders this factor vanish. Then loop 3, 4 decouple from the rest two loops, and in the expansion

$$R_{4,2}(\varepsilon) = R_{4,2}(0) + O(\varepsilon) \tag{2.5}$$

where the additional subscript 2 of R_4 denotes removing two loops at a time, we find

$$R_{4,2}(0) = \frac{s_3\,(x_2 z_1 + x_1 z_2) + (2 s_6 + s_7)(y_2 w_1 + y_1 w_2)}{D_{12}}, \tag{2.6}$$

which equals R_2 when $s_3 = s_6 = 1$ and $s_7 = -1$. This is also easy to understand diagrammatically, and the interesting combination $(2s_6 + s_7)$ explains why we need a minus sign for the cross topology T_7: the block removal of loop 3, 4 of two different orientations of T_6 gives the same 2-loop diagram, therefore one must be eliminated in order to maintain $R_{4,2}(0) = R_2$ while all orientations of T_6 and T_7 are used exactly once, as shown in Fig. 4. This cancelation mechanism is somehow analogous to the cancelation between the cross and the brick-wall patterns in Mondrian diagrammatics [5], and we will see more examples at higher loop orders reflecting the same essence.

Now only s_8 awaits to be explained and we must use the corner removal to detect this non-Mondrian topology T_8, since it has no rectangle or block to be properly removed. Similarly, for removing loop 4 we impose the limit

$$x_4 = y_4 = \frac{1}{\varepsilon}, \quad z_4 = w_4 = 0, \tag{2.7}$$

then in the expansion $R_4(\varepsilon) = R_4(0) + O(\varepsilon)$, we find

$$R_4(0) - R_3 \propto 1 + s_8, \tag{2.8}$$

to maintain the consistency we must take $s_8 = -1$. This is easy to understand if we look at T_4, T_8 together among others, as the D_{ij} factor in the numerator of T_4's integrand requires a counter term for producing the correct Mondrian factor. More concretely, in the 1st line of Fig. 5, the relevant two diagrams give

$$\frac{x_2 x_3 x_4 z_1 z_2 z_3\, y_3 w_2}{D_{12} D_{13} D_{23} D_{24} D_{34}}\,(D_{14} - y_4 w_1) = \frac{z_2}{z_2 + w_2}\,\frac{z_3}{z_3 + w_3} \times \frac{x_2 x_3 z_1^2\, y_3 w_2}{D_{12} D_{13} D_{23}} + O(\varepsilon) \tag{2.9}$$

after using

$$D_{14} - y_4 w_1 = \frac{1}{\varepsilon}\,(z_1 + w_1) - \frac{1}{\varepsilon}\,w_1 = \frac{1}{\varepsilon}\,z_1, \tag{2.10}$$

where

$$\frac{z_2}{z_2 + w_2} \frac{z_3}{z_3 + w_3} = X_2 X_3 \tag{2.11}$$

is the desired Mondrian factor, which characterizes the contacting relation between loop 4 in the diagram of topology T_4 and its 3-loop sub-diagram (or the resulting 3-loop diagram at the RHS).

Moreover, the cancelation between T_6 and T_7 in the 4-loop corner removal $R_4 \to R_3$ again holds, as the relevant three diagrams in the 2nd line of Fig. 5 lead to the combination

$$x_4 z_1 + y_4 w_1 - D_{14} = \frac{1}{\varepsilon} z_1 + \frac{1}{\varepsilon} w_1 - \frac{1}{\varepsilon} (z_1 + w_1) = 0, \tag{2.12}$$

which is exactly isomorphic to the cancelation between the cross and the brick-wall patterns in Mondrian diagrammatics [5].

Let's summarize the nontrivialities in the 4-loop case via understanding $s_1, \ldots, s_8$. First, it is useful to generalize the rectangle removal to the block removal, in order to check the consistency of decoupling more than one loop at a time. At 6-loop order we will also need the block removal of three loops, and so on. Next, topologies T_7, T_8 with coefficient -1 serve as counter terms of those with $+1$, and while T_7 has a clear meaning in Mondrian diagrammatics, T_8 appears to be the necessary *company* of T_4 which has a nontrivial D_{ij} factor in its integrand. At 5-loop order and higher, even a company topology or a group of company topologies will have its further company. While the contributing topologies are more diverse, the overall Mondrian consistency is maintained by these company topologies.

3. Rectangle and block removals at 5-loop

To see more nontrivial examples of various patterns found at $L = 3, 4$, and to check whether new features or exceptions appear, we move on to the 5-loop case. First let's recall the 5-loop DCI topologies as given in Fig. 6, where all 34 topologies are reorganized for later convenience while the same labels used in [6] are kept.

Note that according to the classification in [5], $T_1, \ldots, T_{14}$ are of the ladder type and $T_{17}, \ldots, T_{24}$ are of the cross and brick-wall types. The coefficients or signs of these topologies can be immediately determined by the rule that each cross pattern contributes -1 multiplicatively (otherwise 1), explicitly we have

$$s_1 = s_2 = s_3 = s_4 = s_5 = s_6 = s_7 = s_8 = s_9 = s_{10} = s_{11} = s_{12} = s_{13} = s_{14} = 1, \tag{3.1}$$

$$s_{17} = s_{20} = -1, \quad s_{18} = s_{19} = s_{21} = s_{22} = s_{23} = s_{24} = 1. \tag{3.2}$$

Additionally, each of T_{25}, T_{26} has an obvious attached rectangle, therefore their signs automatically follow that of T_8 in the 4-loop case, namely $s_{25} = s_{26} = -1$.

Upon these inputs, we find the rectangle removal of loop 5

$$x_5 = \frac{1}{\varepsilon}, \quad z_5 = 0 \tag{3.3}$$

leads to $R_5(0) = R_4$ as expected. And the block removal of loop 4, 5

$$x_4 = x_5 = \frac{1}{\varepsilon}, \quad z_4 = z_5 = y_4 = w_5 = 0 \tag{3.4}$$

leads to

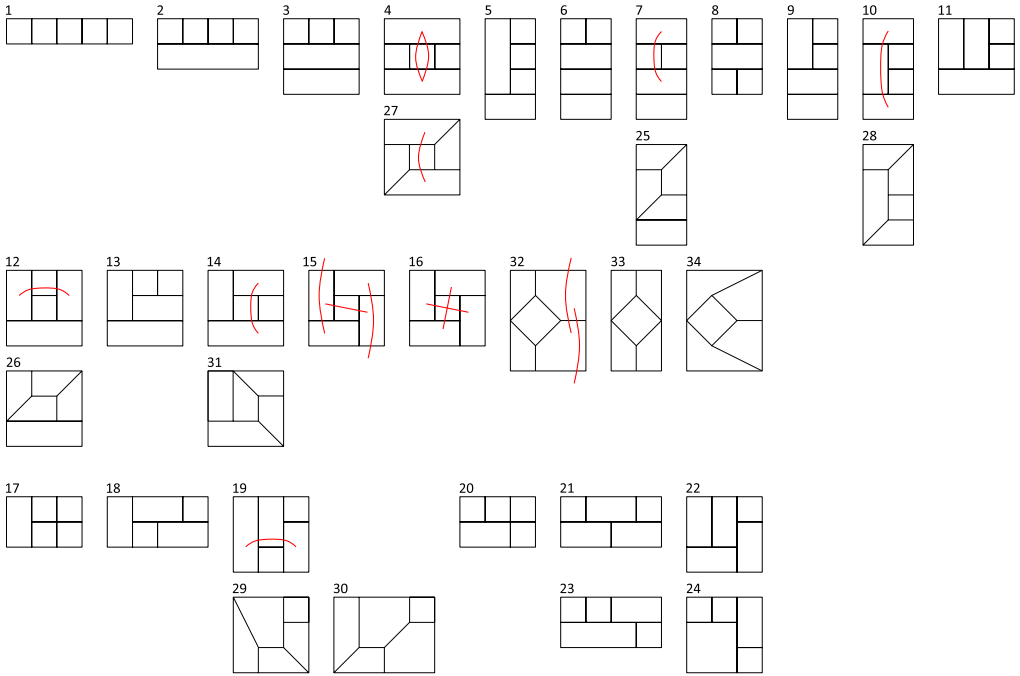$$R_{5,2}(0) - R_3 \propto 2 s_{15} + s_{16} + 2 s_{32} + s_{33}, \tag{3.5}$$

Fig. 6. 5-loop DCI topologies (see [8]). The red curves denote D_{ij} factors, while x, y, z, w factors for T_{15} and T_{32} are also indicated for clarity.
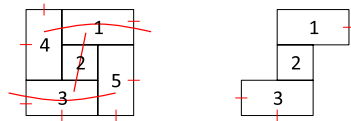

Fig. 7. Identification of s_{15}, s_{16}: removing loop 4,5 with additional cuts on loop 1,3.

which should be zero as required by the consistency. To confirm this guess and to further fully understand the 5-loop case, let's identify s_{15}, s_{16} and $s_{27}, \ldots, s_{34}$ one by one, similar to the identification of s_8 in the 4-loop case.

4. Identifications of the rest coefficients

First of all, s_{28}, s_{29}, s_{30} can be trivially determined by the 4-loop knowledge. Obviously, T_{28} is the company topology of T_{10}, similar to the fact that T_8 is the company topology of T_4 in the 4-loop case, as the T_{10}, T_{28} pair is the counterpart of the T_4, T_8 pair plus one rung. Similarly, T_{29}, T_{30} are the company topologies of T_{19}, note that T_{29} has one rung rule factor and T_{30} has two substitution rule factors which result from the corresponding rung rule factor of T_{19}. Therefore we simply have $s_{28} = s_{29} = s_{30} = -1$.

Now let's consider s_{15}, s_{16} which are a bit tricky. To separate s_{15}, s_{16} from other unknown coefficients, we impose as many cuts as possible around the rim of a particular T_{15} diagram, as shown in Fig. 7, and then use a special two-step expansion. To disentangle s_{15} and s_{16}, we also
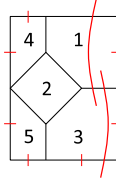
Fig. 8. Identification of s_{31}, s_{32}, s_{33}: removing loop 4,5 with additional cuts on loop 1,3.

relax one external cut, namely $y_1 = 0$ here, and the reason to do so will be clear shortly. Explicitly, we impose the limit

$$x_5 = z_4 = \frac{1}{\varepsilon_1}, \quad y_5 = w_4 = \frac{1}{\varepsilon_2}, \quad y_4 = x_4 = x_3 = w_3 = w_5 = z_5 = z_1 = 0, \tag{4.1}$$

then in the two-step expansion (note the order of expansions matters as we intentionally utilize the x_5, z_4 factors of this diagram to separate it from other sub-leading contributions)

$$R_5'(\varepsilon_1, \varepsilon_2) = R_5'(0, \varepsilon_2) + O(\varepsilon_1), \quad R_5'(0, \varepsilon_2) = R_5'(0, 0) + O(\varepsilon_2), \tag{4.2}$$

where the prime denotes additional cuts $x_3 = w_3 = z_1 = 0$ besides removing loop 4,5 as indicated in Fig. 7, we find

$$R_5'(0, 0) - R_3' \propto (s_{15} + s_{16}) y_1 w_1 - (2 s_{15} + s_{16} - 1) y_3 w_1 - (2 s_{15} + s_{16} + 2 s_{32} + s_{33}) x_1 z_3. \tag{4.3}$$

To maintain the consistency we must have $s_{15} + s_{16} = 0$ and $2s_{15} + s_{16} = 1$, so $s_{15} = 1$ and $s_{16} = -1$, which explains why y_1 must be non-vanishing, otherwise we cannot identify s_{15}, s_{16} with merely $2s_{15} + s_{16} = 1$. As we have assumed $2s_{15} + s_{16} + 2s_{32} + s_{33} = 0$ in the previous section, this condition reduces to $2s_{32} + s_{33} = -1$ which awaits to be confirmed.

Next, we can identify s_{31}, s_{32}, s_{33} upon the inputs of s_{15}, s_{16}, s_{30} in a similar way. Picking a particular T_{32} diagram as given in Fig. 8, we impose the limit

$$z_4 = w_4 = z_5 = y_5 = \frac{1}{\varepsilon}, \quad y_4 = x_4 = x_5 = w_5 = w_3 = z_3 = z_1 = 0, \tag{4.4}$$

and note the external cut of y_1 is relaxed, then in the expansion $R_5'(\varepsilon) = R_5'(0) + O(\varepsilon)$ we find

$$R_5'(0) - R_3' \propto (1 + s_{31}) x_2 x_3 y_1 + (s_{32} + s_{33}) x_2 y_1 (x_3 - w_1)$$
$$+ (1 + 2 s_{32} + s_{33}) x_2 (x_1 x_3 + y_3 w_1), \tag{4.5}$$

so the consistency requires $s_{31} = s_{32} = -1$ and $s_{33} = 1$. Again, y_1 must be non-vanishing, otherwise we can merely know one condition. Now we have confirmed $2s_{32} + s_{33} = -1$ and hence $2s_{15} + s_{16} + 2s_{32} + s_{33} = 0$.

Then for s_{27}, we can pick a particular T_{27} diagram as given in Fig. 9 and impose the limit

$$z_4 = w_4 = x_5 = y_5 = \frac{1}{\varepsilon}, \quad y_1 = y_4 = x_4 = w_3 = w_5 = z_5 = 0, \tag{4.6}$$

now upon the inputs of s_{15}, s_{16} and $s_{28}, \ldots, s_{33}$, we find

$$R_5'(0) - R_3' \propto 1 + s_{27}, \tag{4.7}$$
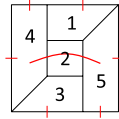
therefore $s_{27} = -1$.

Fig. 9. Identification of s_{27}: removing loop 4,5 with additional cuts on loop 1,3.
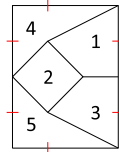

Fig. 10. Identification of s_{34}: removing loop 4,5 with additional cuts on loop 1,3.

Finally for s_{34}, we can pick a particular T_{34} diagram as given in Fig. 10 and impose the limit

$$z_4 = w_4 = z_5 = y_5 = \frac{1}{\varepsilon}, \quad y_4 = x_4 = x_5 = w_5 = z_3 = z_1 = 0, \tag{4.8}$$

upon the inputs of s_{15}, s_{16} and $s_{30}, \ldots, s_{33}$ we find

$$R_5'(0) - R_3' \propto s_{34} - 1, \tag{4.9}$$

therefore $s_{34} = 1$. In summary, in this section we have proved that

$$s_{15} = 1, \quad s_{16} = -1, \quad s_{27} = s_{28} = s_{29} = s_{30} = s_{31} = s_{32} = -1, \quad s_{33} = s_{34} = 1, \tag{4.10}$$

together with the previous section, all 34 coefficients of 5-loop DCI topologies are now identified.

5. Nontrivial Mondrian diagrammatic relations at 5-loop

Knowing all these coefficients, we then proceed further to understand them, for example, why a coefficient is -1 instead of 1, which should not be just an incidental result of imposing cuts at either zero or infinity. Once we find the Mondrian interconnections among various DCI topologies, their coefficients will become a natural consequence of these simple relations extracted from the previous derivations.

More concretely, we would like to explain the universal decoupling relation using one corner removal, which, unlike the rectangle or block removal, can cover all topologies. The limit to be imposed is simple:

$$x_5 = y_5 = \frac{1}{\varepsilon}, \quad z_5 = w_5 = 0, \tag{5.1}$$

namely removing loop 5, then in the expansion $R_5(\varepsilon) = R_5(0) + O(\varepsilon)$ we find $R_5(0) = R_4$. However, this is not the end of the story since $R_5(0) = R_4$ is a redundant relation and it can be further dissected into many much more transparent sub-relations, as diagrammatically shown in Figs. 11 and 12.

In Fig. 11, all nontrivial corner removals of 5-loop DCI topologies are indicated. We will focus on groups of corners denoted by $1, \ldots, 7$, while groups denoted by $A, \ldots, F$ are the direct extensions of the corner removals of T_4, T_8 in the 4-loop case (see Fig. 5). The rest unmentioned
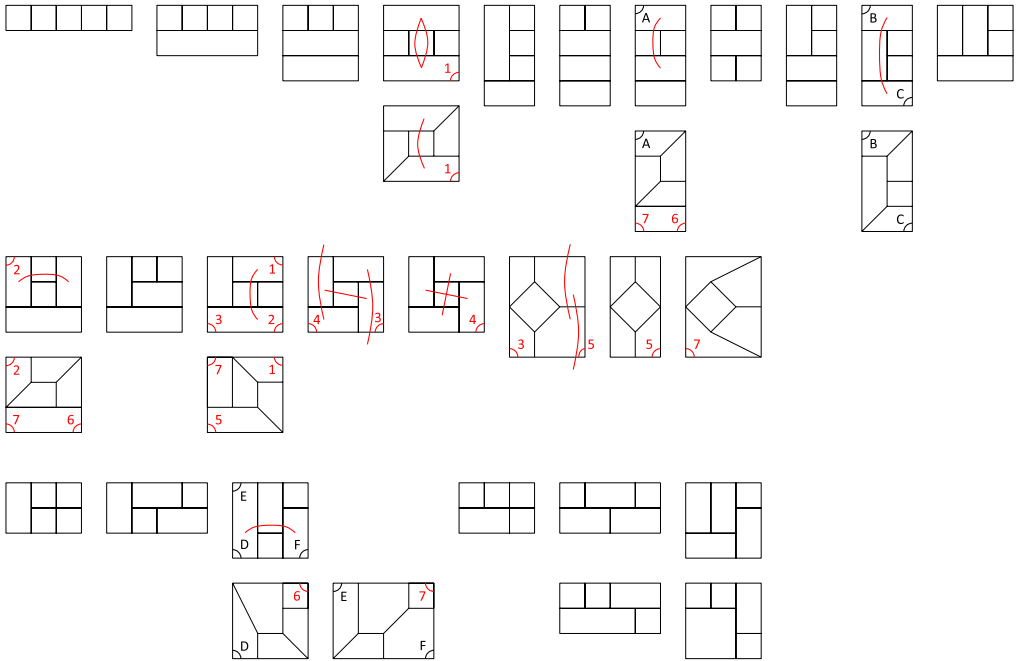
Fig. 11. Nontrivial corners of 5-loop DCI topologies. Groups $A, \ldots, F$ in black denote relations that are direct extensions of the 4-loop case. Groups $1, \ldots, 7$ in red denote new relations at 5-loop.

corners are as trivial as the 3-loop corners or 4-loop corners except those of T_4, T_8, as they locate in visually Mondrian topologies and do not involve the D_{ij} factor.

In Fig. 12, groups $1, \ldots, 7$ are further separated into three types so that we can more clearly understand their nontrivialities, let's select one example from each type to elaborate these delicate relations. In the 1st diagrammatic equality, the 1st and 3rd diagrams have Mondrian pole structures, and in these two diagrams the removed loop has horizontal contacts with loop 1,2 while its contact with the unlabeled loop on top of loop 1 is horizontal in the 1st diagram and vertical in the 3rd. Naively this should give

$$X_1 X_2 X_3 + X_1 X_2 Y_3 = X_1 X_2 D_3 = X_1 X_2 \tag{5.2}$$

according to the definitions in (1.17), which uses a Mondrian completeness relation and here 3 denotes the unlabeled loop. However, the D_{ij} factors in the 1st and 3rd diagrams complicate this relation and that's why we also need the 2nd and 4th diagrams with minus signs to offset that, then we can exactly get the neat result at the RHS with Mondrian factor $X_1 X_2$. The 2nd and 3rd diagrammatic equalities share the same feature of needing non-Mondrian company topologies, to offset the extra complexity brought by the D_{ij} factors. However, such a company topology does not have one-to-one correspondence to a particular Mondrian topology, unlike the T_4, T_8 pair at 4-loop.

For the 4th diagrammatic equality, under the corner removal, schematically it is proportional to $X + Y - D$, so it simply vanishes. The 5th equality follows exactly the same cancelation mechanism, though it is not so obvious as the 4th.

For the 6th diagrammatic equality, under the corner removal three non-Mondrian diagrams sum to a 4-loop non-Mondrian diagram, due to
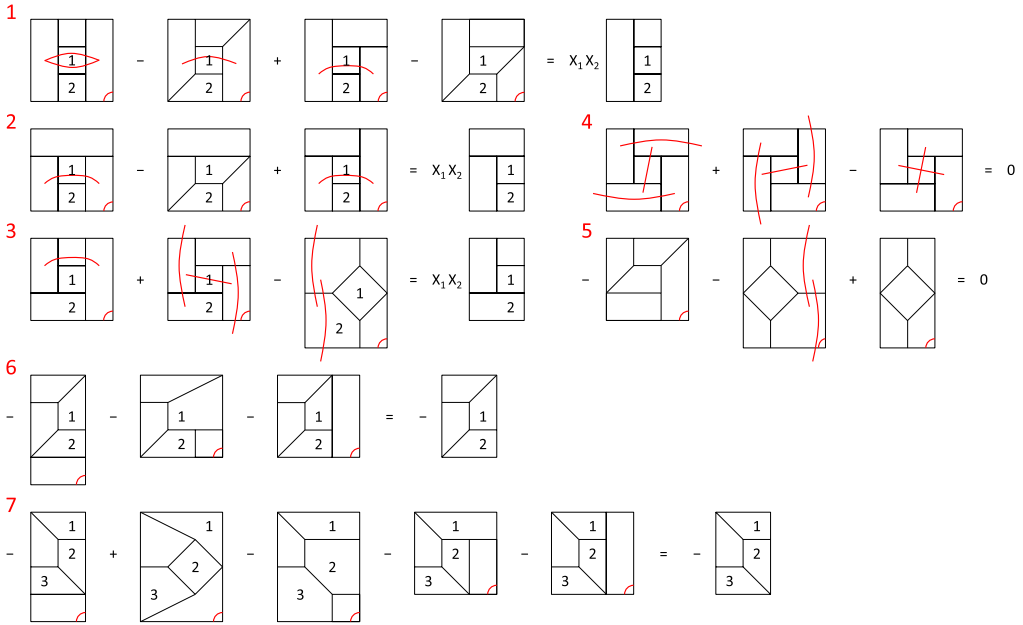
Fig. 12. New Mondrian diagrammatic relations at 5-loop: groups 1, 2, 3 are the relations with obvious Mondrian pole structures, groups 4, 5 are the vanishing or canceling relations and groups 6, 7 are the relations of non-Mondrian company topologies.
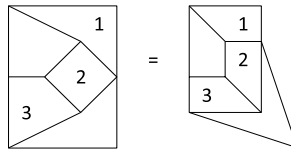

Fig. 13. Deformation to manifest Mondrian factor $D_1 X_2 Y_3$.

$$D_1 Y_2 + Y_1 X_2 + X_1 X_2 = D_1 D_2 = 1. \tag{5.3}$$

Though the resulting 4-loop diagram is not Mondrian, its contact with the 5th loop is still Mondrian, so that we can use the Mondrian completeness relation. The 7th equality is similar but more nontrivial as

$$D_1 D_2 Y_3 - D_1 X_2 Y_3 + D_1 Y_2 X_3 + Y_1 X_2 D_3 + X_1 X_2 D_3 = D_1 D_2 D_3 = 1, \tag{5.4}$$

note the 2nd diagram has a plus sign so it contributes a minus in the Mondrian completeness relation, as the resulting 4-loop diagram also has a minus sign. The Mondrian factor $D_1 X_2 Y_3$ from this diagram is not obvious in the sense of horizontal and vertical contacts, but we can deform its external profile to manifest this, as shown in Fig. 13. Now the external profile of this 5-loop diagram is not a rectangle, but we can see a familiar 4-loop non-Mondrian diagram hidden in it. With Mondrian factor $D_1 X_2 Y_3$ clarified, which is the desired result for offsetting two $D_1 X_2 Y_3$ factors from the rest four diagrams, we see the Mondrian diagrammatics works more effectively than naive visual intuition. A final remark is, the 2nd diagram also serves as a company topology of the rest four, similar to the complexity of the first three identities.
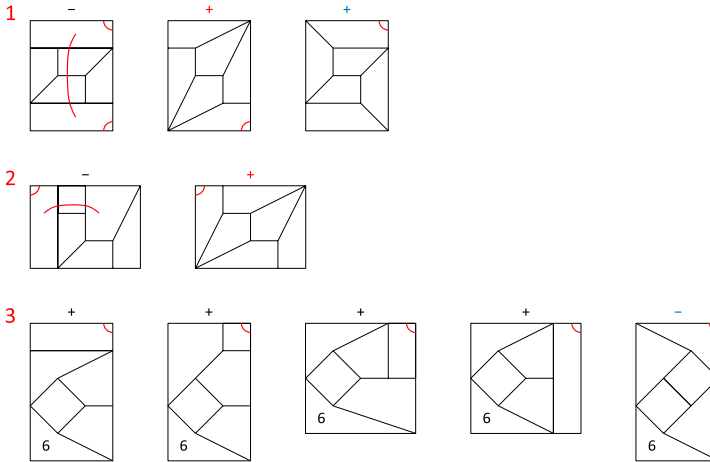
Fig. 14. The two plus signs in red of the first topology add up to $+2$, while the plus and minus signs in blue of the second topology add up to 0, in three relevant Mondrian diagrammatic relations.

6. Coefficients $+2$ and 0 at 6-loop

Finally we can take a glance at the 6-loop case, by investigating the coefficients of two special 6-loop DCI topologies. First of all, the 6-loop amplituhedron or integrand involves 229 non-vanishing contributions of DCI topologies, among which 125 have Mondrian pole structures as listed in Appendix B of [5], while the rest 104 non-Mondrian ones are the company topologies in the sense of corner removal. Interestingly, we also need six vanishing DCI topologies, namely those with coefficient 0, for a complete understanding of the 6-loop corner removal. All these topologies with coefficients can be found in the original result [9].

Similar to the 5-loop case we have extensively described, the new Mondrian diagrammatic relations at 6-loop also can be separated into three types: those with obvious Mondrian pole structures, the vanishing or canceling ones and those of non-Mondrian company topologies. Now we consider two particular 6-loop DCI topologies with three relevant Mondrian diagrammatic relations, as shown in Fig. 14.

The first topology is the 2nd diagram in the 1st relation, or the 2nd diagram in the 2nd relation, as each of them serves as a company topology of the 1st diagram in the 1st or 2nd relation, following exactly the same mechanism of T_4, T_8 pair at 4-loop (see Fig. 5). Since this topology appears twice and in both situations it has a plus sign, its overall coefficient is simply $+2$ as we add up these two pluses!

Similarly, the second topology is the 3rd diagram in the 1st relation, as a company topology for the other corner of the 1st diagram, or the 5th diagram in the 3rd relation, and note that they belong to the same topology though drawn differently. In these two situations it has a plus and a minus respectively, so they cancel and its overall coefficient is 0! One may find the 3rd relation unfamiliar, but it is simply the 7th relation in Fig. 12 if we remove the 6th loop as indicated in Fig. 14. Imagine the deformation in Fig. 13 to better visualize this analogy, one will find this 6-loop relation completely trivial based on its 5-loop counterpart with an overall sign reverse for all topologies. Then the two special coefficients $+2$ and 0 are neatly explained, and the 0's of other 6-loop DCI topologies have similar origins (while there is only one 6-loop DCI topology with coefficient $+2$).

7. Conclusion and outlook

Through substantial examples of DCI integrals at $L = 3, 4, 5, 6$, we discover new interconnections among 4-particle amplituhedra of different loop orders, the latter are defined by $L(L-1)/2$ conditions

$$D_{ij} = (x_j - x_i)(z_i - z_j) + (y_j - y_i)(w_i - w_j) > 0, \tag{7.1}$$

which are symmetric up to all loops. For a higher loop amplituhedron, we can use rectangle, block and corner removals to trivialize $D_{ij} > 0$ conditions involving one or more sets of loop variables (x_i, y_i, z_i, w_i), so it can reduce to a lower loop one. In this way, we can establish a global view of the all-loop 4-particle amplituhedron, in particular, we find the coefficients of DCI integrals of different loop orders which seem to be independent, in fact follow an "inheriting" pattern and it can explain many ± 1 coefficients. Also at the same loop order, coefficients of different DCI topologies are constrained by the simple combinatorial rule: the Mondrian completeness relation. Its underlying mathematics is to repeatedly use $D = X + Y$, as D, X, Y characterize the contacting relations between the removed loop and other loops. To ensure this completeness relation, we also need non-Mondrian (company) DCI topologies as counter terms.

The integration of the all-loop consistency of 4-particle amplituhedron and Mondrian diagrammatics can explain all coefficients of DCI topologies at $L = 3, 4, 5, 6$, providing a more transparent supplementary understanding of the results generated by the soft-collinear bootstrap [9]. Its simplicity results from the definition of amplituhedron with its properties under certain limits, and it is an desirable future direction to develop an equally simple direct construction of the basis of DCI integrals based on this insight.

Historically, since the well known rung rule at 2-loop order [10], there have been various rules relating L-loop and $(L+1)$-loop amplitudes. Besides the algebraic approach [9] above which imposes the correct soft-behavior of the logarithm of the amplitude, they also include the correlator-inspired relations used in [11] which generalize the rung rule and introduce other rules, and the square plus triangle rules in [13]. It is interesting to note that there are some graphical similarities between the square plus triangle rules and the rectangle (block) plus corner rules. However, mathematically they appear to be quite different at the current stage of understanding, as the physical meanings of, for example, positive infinity and Mondrian completeness relation await to be explored. We would like to again emphasize that, at least up to 6-loop, the corner removal alone can account for all coefficients.

At 7-loop order there is no novelty other than $+2$ and 0 coefficients [9], while starting from the 8-loop case fractional coefficients begin to appear [12,13]. Therefore we expect a nontrivial generalization of the Mondrian diagrammatic relations at $L \geq 8$, but they should be not too exotic since these coefficients are still rational. Finally, we would like to explore how the Mondrian consistency connecting amplituhedra of different loop orders can be extended to the generic case of more than four particles [3,14,15], and what it can tell us about the generic case from the 4-particle knowledge [16].

Declaration of competing interest

The authors declare that they have no known competing financial interests or personal relationships that could have appeared to influence the work reported in this paper.

References

[1] N. Arkani-Hamed, J. Trnka, The amplituhedron, J. High Energy Phys. 1410 (2014) 030, arXiv:1312.2007 [hep-th].

[2] N. Arkani-Hamed, J. Trnka, Into the amplituhedron, J. High Energy Phys. 1412 (2014) 182, arXiv:1312.7878 [hep-th].

[3] N. Arkani-Hamed, H. Thomas, J. Trnka, Unwinding the amplituhedron in binary, J. High Energy Phys. 1801 (2018) 016, arXiv:1704.05069 [hep-th].

[4] J. Rao, 4-particle amplituhedron at 3-loop and its Mondrian diagrammatic implication, J. High Energy Phys. 1806 (2018) 038, arXiv:1712.09990 [hep-th].

[5] Y. An, Y. Li, Z. Li, J. Rao, All-loop Mondrian diagrammatics and 4-particle amplituhedron, J. High Energy Phys. 1806 (2018) 023, arXiv:1712.09994 [hep-th].

[6] J. Rao, 4-particle amplituhedronics for 3-5 loops, Nucl. Phys. B 943 (2019) 114625, arXiv:1806.01765 [hep-th].

[7] Z. Bern, M. Czakon, L.J. Dixon, D.A. Kosower, V.A. Smirnov, The four-loop planar amplitude and cusp anomalous dimension in maximally supersymmetric Yang-Mills theory, Phys. Rev. D 75 (2007) 085010, arXiv:hep-th/0610248.

[8] Z. Bern, J.J.M. Carrasco, H. Johansson, D.A. Kosower, Maximally supersymmetric planar Yang-Mills amplitudes at five loops, Phys. Rev. D 76 (2007) 125020, arXiv:0705.1864 [hep-th].

[9] J.L. Bourjaily, A. DiRe, A. Shaikh, M. Spradlin, A. Volovich, The soft-collinear bootstrap: N=4 Yang-Mills amplitudes at six and seven loops, J. High Energy Phys. 1203 (2012) 032, arXiv:1112.6432 [hep-th].

[10] Z. Bern, J. Rozowsky, B. Yan, Two loop four gluon amplitudes in N=4 superYang-Mills, Phys. Lett. B 401 (1997) 273–282, arXiv:hep-ph/9702424 [hep-ph].

[11] B. Eden, P. Heslop, G.P. Korchemsky, E. Sokatchev, Constructing the correlation function of four stress-tensor multiplets and the four-particle amplitude in N=4 SYM, Nucl. Phys. B 862 (2012) 450, arXiv:1201.5329 [hep-th].

[12] J.L. Bourjaily, P. Heslop, V.V. Tran, Perturbation theory at eight loops: novel structures and the breakdown of manifest conformality in N=4 supersymmetric Yang-Mills theory, Phys. Rev. Lett. 116 (19) (2016) 191602, arXiv:1512.07912 [hep-th].

[13] J.L. Bourjaily, P. Heslop, V.V. Tran, Amplitudes and correlators to ten loops using simple, graphical bootstraps, J. High Energy Phys. 1611 (2016) 125, arXiv:1609.00007 [hep-th].

[14] N. Arkani-Hamed, C. Langer, A. Yelleshpur Srikant, J. Trnka, Deep into the amplituhedron: amplitude singularities at all loops and legs, Phys. Rev. Lett. 122 (5) (2019) 051601, arXiv:1810.08208 [hep-th].

[15] R. Kojima, Triangulation of 2-loop MHV amplituhedron from sign flips, J. High Energy Phys. 1904 (2019) 085, arXiv:1812.01822 [hep-th].

[16] P. Heslop, V.V. Tran, Multi-particle amplitudes from the four-point correlator in planar $\mathcal{N} = 4$ SYM, J. High Energy Phys. 1807 (2018) 068, arXiv:1803.11491 [hep-th].